

# Spillover in monomer–monomer reactions on supported catalysts: dynamic mean-field study

V. Skakauskas · P. Katauskis

Received: 4 November 2013 / Accepted: 23 January 2014 / Published online: 5 February 2014  
© Springer International Publishing Switzerland 2014

**Abstract** The kinetics of a  $A_1 + A_2 \rightarrow A_1A_2$  reaction on supported catalysts is investigated numerically using a phenomenological model which includes: the bulk diffusion of reactants from a bounded vessel towards the adsorbent and the product bulk one into the same vessel, adsorption and desorption of reactants molecules, and surface diffusion of adsorbed particles. The model is based on the Langmuir–Hinshelwood surface reaction mechanism coupled with the Eley–Rideal step. The model based only on the Langmuir–Hinshelwood mechanism is also studied. Simulations were performed using the finite difference technique. Three cases of reactants adsorption are considered: each reactant can adsorb on the active in reaction catalyst surface and inactive support, one of reactants adsorbs on the catalyst surface while the other one adsorbs on the support, both reactants adsorb only on the support. The surface diffusion and catalytic surface size influence on the catalytic reactivity of a supported catalyst is studied.

**Keywords** Heterogeneous reactions · Adsorption · Desorption · Surface diffusion · Spillover

## 1 Introduction

Heterogeneous catalytic reactions constitute around 90 % of all processes in the chemical industry [1]. Modelling of catalytic processes plays a central role in study of kinetics in heterogeneous catalysis and catalysts design in chemical industry [1–5]. The rate constants of kinetic processes are usually obtained either from single crystal studies

---

V. Skakauskas (✉) · P. Katauskis  
Faculty of Mathematics and Informatics, Vilnius University,  
Naugarduko 24, 03225 Vilnius, Lithuania  
e-mail: vladaskakauskas@maf.vu.lt

or experimentally from real catalysts [6]. The latter consist of small active catalyst particles placed on inactive in reaction supports. One of kinetic effects associated with small catalyst particles on a support is the spillover effect. Spillover is an effect accompanying heterogeneous surface reactions when inactive in reactions surface regions significantly influence the kinetics of the overall catalytic process [7]. It is caused by the fact that parts of the surface which are inactive in the surface reaction can be active for other processes that occur during the catalytic process, i.e. adsorption–desorption process and increase or decrease concentrations of either substrate or product particles on active parts of the surface through the diffusion of the adsorbed reactant particles across the interface between the catalyst particles and the support [1, 7, 8]. The term “spillover” originally was used only for diffusion from active in reaction particles onto a support, whereas the diffusion in reverse direction is called “reverse-spillover” [4, 9–11]. In the present paper the term spillover will be used for diffusion in both directions. The spillover effect is observed and plays a key role in catalytic reactions on supported metal catalysts [4, 9]. The bibliography of the current state of theoretical research of reactions with spillover effects include: experimental works [12–19], papers based on the Monte Carlo simulations technique [7, 9, 20, 21], numerical solving of mean-field models [22–25], and the analytical description of such effect [2, 6]. In [20], the uni-molecular  $A \rightarrow B$  and bimolecular  $2A \rightarrow B$  reversible reactions are studied on heterogeneous surfaces consisting of active and inactive in reaction sites.

In [7, 9, 21], the three-molecular  $2A + B_2 \rightarrow 2AB$  reaction which models the CO oxidation on Pd/Al<sub>2</sub>O<sub>3</sub> heterogeneous catalyst, is studied. In [22, 23], these reactions are studied numerically by using mean-field equations for the steady-state case. The long-range surface diffusion influence on the uni-molecular reactions proceeding on the heterogeneous catalysts is studied numerically in [24, 25]. Under some restrictions on rate constants and ratio of reactants pressures authors of [2] derived approximate analytical formulas to describe dynamics of  $2A + B_2 \rightarrow 2AB$  reaction with spillover effect. Using analytical methods and scaling concepts a model for steady-state uni-molecular reactions on supported catalysts including reactant adsorption, desorption, and diffusion of adsorbed particles is examined in [1].

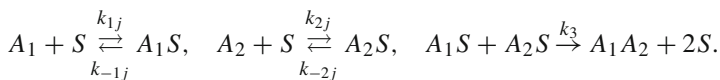
In this paper, by employing a mean-field model and its numerical simulations we consider a monomer–monomer heterogeneous reaction,  $A_1 + A_2 \rightarrow B$ ,  $B = A_1A_2$ , on a supported (composite) catalyst taking into account: the bulk diffusion of both reactants from a bounded vessel with an impermeable boundary toward the adsorbent and the reaction product bulk one from the adsorbent into the same vessel, adsorption, desorption, and surface diffusion of adsorbed particles of each reactant. The model is based on the Langmuir–Hinshelwood surface reaction mechanism coupled with the Eley–Rideal step. In particular, the model based only on the Langmuir–Hinshelwood mechanism is studied. Adsorption, desorption, and surface diffusion are allowed to proceed at a constant temperature and the product desorption is assumed to be instantaneous. We consider three adsorption cases of reactants  $A_1$  and  $A_2$ : (i) each reactant can adsorb on both active catalyst particle and inactive support, (ii) one of reactants  $A_1$  and  $A_2$  adsorbs on the catalyst particle while the other one adsorbs on the inactive in reaction support, (iii) both reactants adsorb only on the inactive support. The goal of this paper is a numerical study of the surface diffusion and catalytic particle size influence on the catalytic reactivity of supported catalysts.

The paper is organized as follows. In Sect. 2 we present the model. In Sect. 3 we discuss numerical results. A summary of main results in Sect. 4 concludes the paper.

## 2 The model

To study the problem of two-molecular catalytic heterogeneous reaction,  $A_1 + A_2 \rightarrow B$ , proceeding on a supported catalyst we use a mean-field approach. Assume that reactants  $A_1$ ,  $A_2$  and product  $B = A_1A_2$  of concentrations  $a_1(t, x)$ ,  $a_2(t, x)$ , and  $b(t, x)$  occupy a bounded domain  $\Omega = \{x = (x_1, x_2, x_3) : x_i \in [0, l], i = 1, 2, 3\}$  with boundary  $\tilde{S} = S_1 \cup S_2$ , where  $S_2 = \{x = (x_1, x_2, x_3) : x_i \in [0, l], i = 1, 3, x_2 = 0\}$  and  $S_1 = \tilde{S} \setminus S_2$ . Here  $t$  is time,  $x$  is a position,  $S_2$  is the surface of the adsorbent, and  $S_1$  is a surface impermeable to the reactants and product. Obviously,  $x_2 > 0$  for  $S_1$ . Let  $s_2(x)$  and  $s_1(x)$ ,  $x = (x_1, x_3) \in S_2$ , be the surface densities of the active and inactive sites in the surface reaction, respectively. Assume that  $u_{i2} = s_2\theta_{i2}$  and  $u_{i1} = s_1\theta_{i1}$ ,  $\theta_{ij}(t, x) \in [0, 1]$ ,  $j = 1, 2$ , are the densities of the active and inactive in reaction sites occupied by the adsorbed molecules of reactant  $A_i$ ,  $i = 1, 2$ . Then  $s_j(1 - \theta_{ij})$ ,  $i, j = 1, 2$ , are the densities of the free sites. Since according to Langmuir one molecule adsorbs on only one adsorption site, function  $u_{ij}$  also present density of molecules of reactant  $A_i$  adsorbed on sites of type  $j$  ( $j = 1$  for inactive sites,  $j = 2$  for active ones) that are located at point  $x$ . Assume that  $S_2 = S_{22} \cup S_{21}$  where  $S_{22} = \{(x_1, x_2, x_3) : x_1 \in [0, x_*], x_2 = 0, x_3 \in [0, l]\}$  and  $S_{21} = \{(x_1, x_2, x_3) : x_1 \in (x_*, l], x_2 = 0, x_3 \in [0, l]\}$ ,  $x_* \in (0, l)$ , are planes consisting of the active and inactive sites, respectively. Let  $k_{ij}$  and  $k_{-ij}$  be the adsorption and desorption rates constants and let  $\kappa_{ij}$ ,  $i, j = 1, 2$ , be the surface diffusivity of adsorbed particles of reactant  $A_i$  on the surface  $S_{2j}$ . To simplify the model we restrict ourselves to the case where densities  $s_1$  and  $s_2$  depend only on variable  $x_1$  and the initial values  $a_1^0$  and  $a_2^0$  of concentrations  $a_1$  and  $a_2$  are constants. In this case we can reduce the three-dimensional problem into two-dimensional one. Let  $\lambda_{1,i2}$ ,  $i = 1, 2$ , be the constant of the jump rate via the catalyst-support interface  $x_*$  of an adsorbed  $A_i$  particle from the active position  $x_* - 0$  into the nearest-neighbour vacant inactive site  $x_* + 0$ . Similarly, let  $\lambda_{2,i1}$ ,  $i = 1, 2$ , be the constant of the jump rate via the catalyst-support of an adsorbed  $A_i$  particle from the inactive position  $x_* + 0$  into the nearest-neighbour vacant active site  $x_* - 0$ .

To construct the model we employ the Langmuir–Hinshelwood (LH) mechanism



Here  $S$  is the adsorption site and  $k_3$  is the reaction between  $A_1S$  and  $A_2S$  rate constant in LH step. In principle the product  $B = A_1A_2$  formation may occur via one or both Eley–Rideal (ER) steps



where  $k_1$  is the reaction between  $A_1$  and  $A_2S$  rate constant and  $k_2$  is the reaction between  $A_2$  and  $A_1S$  rate one. Assuming that product desorption is instantaneous and employing the LH and ER mechanisms we get the following system for densities  $u_{ij}$ :

$$\begin{cases} \partial_t u_{11} = k_{11}a_1(s_1 - u_{11} - u_{21}) - k_{-11}u_{11} + \kappa_{11} \frac{\partial^2 u_{11}}{\partial x_1^2}, & x_1 \in (x_*, l), \\ \partial_t u_{21} = k_{21}a_2(s_1 - u_{11} - u_{21}) - k_{-21}u_{21} + \kappa_{21} \frac{\partial^2 u_{21}}{\partial x_1^2}, & x_1 \in (x_*, l), \\ \partial_t u_{12} = k_{12}a_1(s_2 - u_{12} - u_{22}) - k_{-12}u_{12} - k_3u_{12}u_{22} - k_2a_2u_{12} \\ \quad + \kappa_{12} \frac{\partial^2 u_{12}}{\partial x_1^2}, & x_1 \in (0, x_*), \\ \partial_t u_{22} = k_{22}a_2(s_2 - u_{12} - u_{22}) - k_{-22}u_{22} - k_3u_{12}u_{22} - k_1a_1u_{22} \\ \quad + \kappa_{22} \frac{\partial^2 u_{22}}{\partial x_1^2}, & x_1 \in (0, x_*), \end{cases} \tag{1}$$

Here  $\partial_t$  signifies the partial derivative with respect to time. We add to this system the initial

$$u_{ij}(0, x_1) = 0, \quad i, j = 1, 2, \tag{2}$$

and boundary conditions at points  $x_1 = 0$ ,  $x_1 = x_*$ , and  $x_1 = l$ ,

$$\begin{cases} \left. \frac{\partial u_{12}}{\partial x_1} \right|_{x_1=0} = \left. \frac{\partial u_{22}}{\partial x_1} \right|_{x_1=0} = 0, \\ \left. \frac{\partial u_{11}}{\partial x_1} \right|_{x_1=l} = \left. \frac{\partial u_{21}}{\partial x_1} \right|_{x_1=l} = 0, \end{cases} \tag{3}$$

$$\begin{cases} \kappa_{11} \left. \frac{\partial u_{11}}{\partial x_1} \right|_{x_*+0} = \kappa_{12} \left. \frac{\partial u_{12}}{\partial x_1} \right|_{x_*-0} = \lambda_{2,11}u_{11}|_{x_*+0}(s_2 - u_{12} - u_{22})|_{x_*-0} \\ \quad - \lambda_{1,12}u_{12}|_{x_*-0}(s_1 - u_{11} - u_{21})|_{x_*+0}, \\ \kappa_{21} \left. \frac{\partial u_{21}}{\partial x_1} \right|_{x_*+0} = \kappa_{22} \left. \frac{\partial u_{22}}{\partial x_1} \right|_{x_*-0} = \lambda_{2,21}u_{21}|_{x_*+0}(s_2 - u_{12} - u_{22})|_{x_*-0} \\ \quad - \lambda_{1,22}u_{22}|_{x_*-0}(s_1 - u_{11} - u_{21})|_{x_*+0}. \end{cases} \tag{4}$$

The first terms (gain fluxes) on the right-hand side of Eq. (4) are conditioned by the jumps via the catalyst-support interface  $x_*$  of the escaped molecules of reactant  $A_i$ ,  $i = 1, 2$ , from the inactive position,  $x_* + 0$ , of the support to the nearest-neighbour vacant active one,  $x_* - 0$ , of the catalyst. Similarly, the other two terms (loss fluxes) on the right-hand side of Eq. (4) are conditioned by the jumps via the catalyst-support interface of the escaped molecules of the same reactant from the active position  $x_* - 0$  of the catalyst to the nearest-neighbour vacant inactive one,  $x_* + 0$ , of the support.

Diffusion of the reactants  $A_1$  and  $A_2$  toward the adsorbent and the product  $B$  from the adsorbent away into the same vessel is described by the systems:

$$\left\{ \begin{array}{l} \partial_t a_1 = \kappa_{a_1} \left( \frac{\partial^2 a_1}{\partial x_1^2} + \frac{\partial^2 a_1}{\partial x_2^2} \right), \quad (x_1, x_2) \in (0, l) \times (0, l), \\ \partial_n a_1|_{S_1} = 0, \\ \partial_n a_1 = -(k_{11}a_1(s_1 - u_{11} - u_{21}) - k_{-11}u_{11})/\kappa_{a_1}, \\ \quad x_1 \in (x_*, l), \quad x_2 = 0, \\ \partial_n a_1 = -(k_{12}a_1(s_2 - u_{12} - u_{22}) - k_{-12}u_{12} + k_{11}a_1u_{22})/\kappa_{a_1}, \\ \quad x_1 \in (0, x_*), \quad x_2 = 0, \\ a_1(0, x) = a_{10}(x), \end{array} \right. \quad (5)$$

$$\left\{ \begin{array}{l} \partial_t a_2 = \kappa_{a_2} \left( \frac{\partial^2 a_2}{\partial x_1^2} + \frac{\partial^2 a_2}{\partial x_2^2} \right), \quad (x_1, x_2) \in (0, l) \times (0, l), \\ \partial_n a_2|_{S_1} = 0, \\ \partial_n a_2 = -(k_{21}a_2(s_1 - u_{11} - u_{21}) - k_{-21}u_{21})/\kappa_{a_2}, \\ \quad x_1 \in (x_*, l), \quad x_2 = 0, \\ \partial_n a_2 = -(k_{22}a_2(s_2 - u_{12} - u_{22}) - k_{-22}u_{22} + k_{21}a_2u_{12})/\kappa_{a_2}, \\ \quad x_1 \in (0, x_*), \quad x_2 = 0, \\ a_2(0, x) = a_{20}(x), \end{array} \right. \quad (6)$$

$$\left\{ \begin{array}{l} \partial_t b = \kappa_b \left( \frac{\partial^2 b}{\partial x_1^2} + \frac{\partial^2 b}{\partial x_2^2} \right), \quad (x_1, x_2) \in (0, l) \times (0, l), \\ \partial_n b|_{S_1} = 0, \\ \partial_n b = (k_3u_{12}u_{22} + k_1a_1u_{22} + k_2a_2u_{12})/\kappa_b, \quad x_1 \in (0, x_*), \quad x_2 = 0, \\ \partial_n b = 0, \quad x_1 \in (x_*, l), \quad x_2 = 0, \\ b(0, x) = 0. \end{array} \right. \quad (7)$$

Here  $\partial_n f$ ,  $f = a_1, a_2, b$ , is the outward normal derivative. System (1)–(7) possesses two conservation laws

$$\int_{\Omega} (a_i + b) dx + \int_0^{x_*} u_{i2} dx_1 + \int_{x_*}^l u_{i1} dx_1 = \int_{\Omega} a_{i0} dx, \quad i = 1, 2. \quad (8)$$

Coupled system (1)–(7) determines densities  $u_{ij}$  (or surface coverages  $\theta_{ij}$ ) for all  $x \in S_2$  and concentrations  $a_1, a_2$ , and  $b$  of reactants  $A_1, A_2$  and product  $B$  for all  $x \in \Omega$  and  $t > 0$ .

We also study system (1)–(4) with given concentrations  $a_1$  and  $a_2$  at the surface  $S_2$ .

The main characteristic that we study is the surface  $S_2$  specific conversion rate of the reactants molecules into the product ones (turn-over rate or turn-over frequency) determined by the formula

$$z = \int_0^{x_*} (k_3 u_{12} u_{22} + k_1 a_1 u_{22} + k_2 a_2 u_{12}) dx_1 / \int_0^{x_*} s_2 dx_1. \tag{9}$$

Using the dimensionless variables  $\bar{t} = t/T$ ,  $\bar{x}_i = x_i/l$ ,  $\bar{a}_i = a_i/a_*$ ,  $\bar{s}_i = s_i/(la_*)$ ,  $\bar{b} = b/a_* \bar{k}_{ij} = k_{ij} T a_*$ ,  $\bar{k}_{-ij} = k_{-ij} T$ ,  $\bar{k}_3 = k_3 T$ ,  $\bar{k}_i = k_i T a_*$ ,  $\bar{\kappa}_{a_i} = \kappa_{a_i} T/l^2$ ,  $\bar{\kappa}_b = \kappa_b T/l^2$ ,  $\bar{\kappa}_{ij} = \kappa_{ij} T/l^2$ ,  $\bar{\lambda}_{1,j2} = a_* T \lambda_{1,j2}$ ,  $\bar{\lambda}_{2,j1} = a_* T \lambda_{2,j1}$ , where  $i, j = 1, 2$  and  $T, l, a_*$  are the characteristic dimensional units, we rewrite Eqs. (1)–(8) in the same form, but in dimensionless variables.

In what follows we study system (1)–(7) and Eqs. (1)–(4) with given values of  $a_1, a_2$  at the surface  $x_2 = 0$  in the following three adsorption cases of the reactants  $A_1$  and  $A_2$ :

- (i) each reactant can adsorb on both intervals  $[0, x_*)$  and  $(x_*, 1]$ ,
- (ii) reactant  $A_2$  adsorbs on the interval  $[0, x_*)$ , while the  $A_1$  adsorbs on the  $(x_*, 1]$ ,
- (iii) both reactants adsorb only on the interval  $(x_*, 1]$ .

Hence, in case (ii) we have  $k_{12} = k_{21} = 0$ , while in the case (iii)  $k_{12} = k_{22} = 0$ .

### 3 Numerical results

System (1)–(4) with given values of  $a_1$  and  $a_2$  at the surface  $S_2$  was solved numerically using an implicit difference scheme. To solve system (1)–(7) numerically we used an implicit difference scheme based on the alternating direction method [26]. For all calculations we used the following dimensional data:

$$\begin{aligned} T &= 1 \text{ s}, \quad l = 10^{-1} \text{ cm}, \quad a_* = 10^{-11} \text{ mol cm}^{-3}, \\ s_* &= l a_* = 10^{-12} \text{ mol cm}^{-2}, \quad k_{ij} \in [10^9, 10^{11}] \text{ cm}^3 \text{ mol}^{-1} \text{ s}^{-1}, \\ k_{-ij}, k &\in [3 \times 10^{-3}, 1] \text{ s}^{-1}, \quad \kappa_{a_i}, \kappa_b \in [5 \times 10^{-7}, 10^{-3}] \text{ cm}^2 \text{ s}^{-1}. \end{aligned} \tag{10}$$

In the case where values of  $k_{ij}, \kappa_{ij}$ , and  $\lambda_{i,jn}$  for all values of indices are equal, we use  $k = k_{ij}, \kappa = \kappa_{ij}$ , and  $\lambda = \lambda_{i,jn}$  for short. Of course, the case where  $k_{ij}, \kappa_{ij}$ , and  $\lambda_{i,jn}$  do not depend on values of indices is not realistic. However, it is useful for a study of the interplay of many different physico-chemical processes. In calculations, we used  $k_3 = 0.1, k_{-ij} = 1.66 \times 10^{-3}$  and two different arrangements of the adsorption sites  $s_1 = s_2 = 1$  and  $s_2 = s_1(1/x_* - 1), s_1 = 1$ . In the first case of the adsorption sites arrangement, the total numbers of the active and inactive sites for  $x_* \neq 0.5$  are different. In the second case, these numbers are equal, i.e.  $\int_0^{x_*} s_2 dx_1 = \int_{x_*}^1 s_1 dx_1$ . Moreover, for  $x_* = 0.5, s_2 = s_1 = 1$  in the second case too. The model values of dimensionless  $k_{ij}, \kappa_{ij}$ , and  $\lambda_{i,jn}$  are given in the captions of figures. We first discuss numerical results for system (1)–(4) with given values of  $a_1$  and  $a_2$  at the surface  $S_2$ .

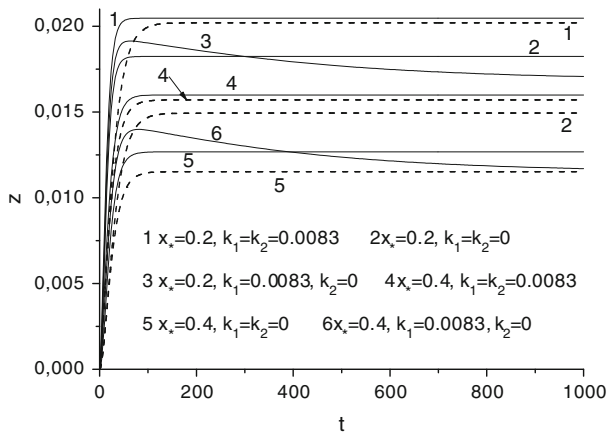


**Fig. 1** Influence of the active interval length  $x_*$  and reaction rate constants,  $k_1$  and  $k_2$ , in ER step on the turnover rate  $z(t)$  determined by Eqs. (1)–(4) with  $a_1 = a_2 = 1$  at the surface  $S_2$  for densities  $s_1 = s_2 = 1$  (dashed line) and  $s_1 = 1, s_2 = s_1(1/x_* - 1)$  (solid line) in the case  $\kappa = 0.5, \lambda = 0.5$ , and  $k = 0.0166$

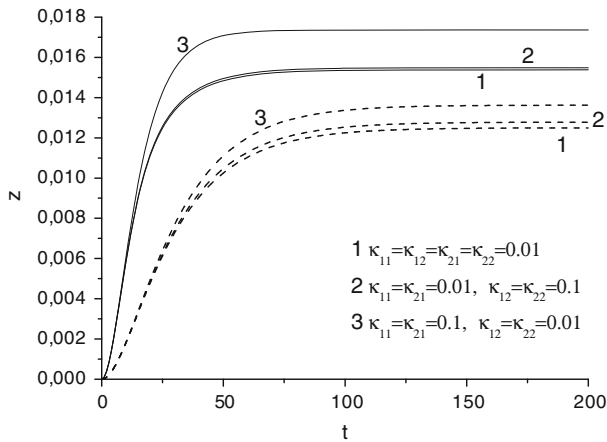


**Fig. 2** Dependence of turnover rate  $z(t)$  determined by (1)–(4) with  $a_1 = a_2 = 1$  at the surface  $S_2$  for densities  $s_1 = s_2 = 1$  (dashed line) and  $s_1 = 1, s_2 = s_1(1/x_* - 1)$  (solid line) on the parameters  $\kappa_{ij}$ ,  $i, j = 1, 2$ , in the case  $\lambda = 0.5, k_1 = k_2 = 0$ , and  $k = 0.0166$

### 3.1 Numerical results of system (1)–(4) with $a_1(t, x_1, 0) = a_2(t, x_1, 0) = 1$

Numerical results are presented in Figs. 1, 2, 3, 4 and 5.

Figure 1 illustrates the dependence of the turn-over rate  $z$  on the parameters  $s_1, s_2, x_*$ , and  $k_1 = k_2$  for the case where  $\kappa = \lambda = 0.5$  and each reactant can adsorb on both active and inactive intervals. In both cases of the  $s_1$  and  $s_2$  arrangement, Fig. 1 depicts a growth of the turn-over rate  $z$  as the size of the active interval,  $x_*$ , decreases (at the same time the length of the inactive interval,  $1 - x_*$ , grows). For uni-molecular reactions this effect is studied in [2]. This figure also shows that incorporation of the ER step for one or both reactants remarkably increases  $z$  compared to that determined by the model involving only the LH mechanism.

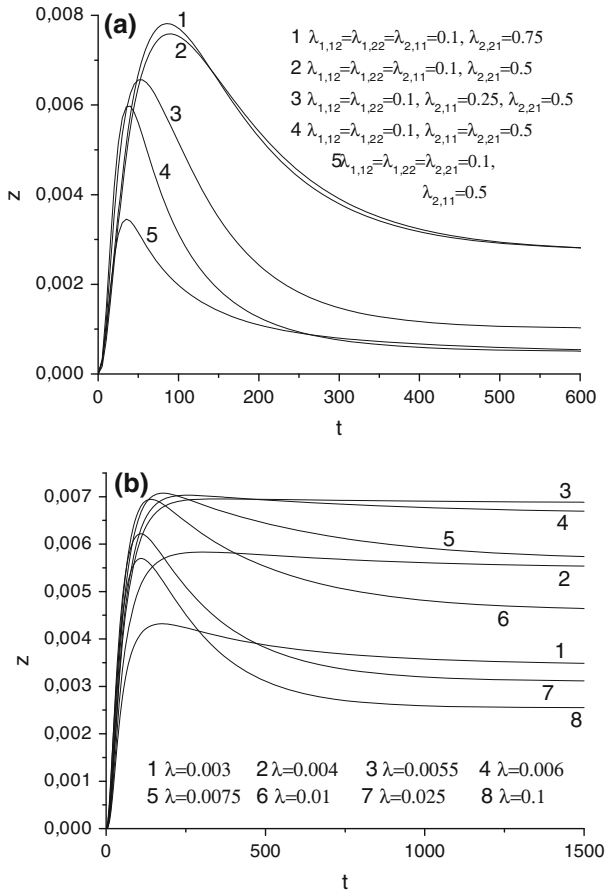


**Fig. 3** Effect of increasing parameters  $\lambda_{i,jn}$  (a) and  $\lambda$  (b) on the turnover rate  $z(t)$  determined by (1)–(4) with  $a_1 = a_2 = 1$  at the surface  $S_2$  in the case  $k_{11} = k_{22} = 0.0166, k_{12} = k_{21} = 0, k_1 = k_2 = 0, \kappa = 0.01$ , and  $s_1 = s_2 = 1$

Figure 2 depicts the influence of the surface diffusivity  $\kappa_{ij}$  on the dynamics of  $z$  for the case where the reactants  $A_1$  and  $A_2$  can adsorb on both active and inactive intervals and  $k = 1.66 \times 10^{-2}, \lambda = 0.1, k_1 = k_2 = 0$ . From this figure we see that in both cases of the distribution of  $s_1$  and  $s_2$  the increase of the diffusivity in the inactive interval,  $\kappa_{11} = \kappa_{21}$ , leads to the larger values of  $z$  compared to those corresponding to the same increase of the diffusivity  $\kappa_{12} = \kappa_{22}$  in the active interval. Figs. 1 and 2 also shows that values of  $z$  for  $s_2 = s_2(1/x_* - 1), s_1 = 1$  are much more larger than those corresponding to the case  $s_1 = s_2 = 1$ .

Figures 3a, b present the dependence of  $z$  on  $\lambda_{i,jn}$  and  $\lambda$ , respectively, for  $\kappa = 0.01, k_1 = k_2 = 0, k_{11} = k_{22} = 1.66 \times 10^{-2}$  in the case where  $A_1$  adsorbs on  $(0, x_*)$  and  $A_2$  on  $(x_*, 1)$ , i.e.  $k_{12} = k_{21} = 0$ . From Fig. 3a we observe that the increase of  $\lambda_{2,21}$  or  $\lambda_{2,11}$  increases values of  $z$  for small  $t$ . For large  $t$  the turn-over rate behaves vice-versa. Figure 3b shows that the steady-state value of  $z$  depending on  $\lambda$  possesses a maximum value at some  $\lambda_*$ , e.g.  $\lambda_* \approx 0.055$ .



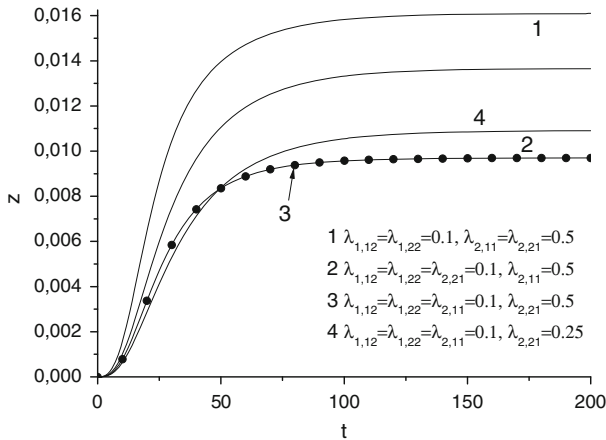


**Fig. 4** Effect of increasing parameters  $\lambda_{i,jn}$  on the turnover rate  $z(t)$  determined by (1)–(4) with  $a_1 = a_2 = 1$  at the surface  $S_2$  for densities  $s_1 = s_2 = 1$  in the case  $k_{11} = k_{21} = 0.0166, k_{12} = k_{22} = 0$ , and  $k_1 = k_2 = 0, \kappa = 0.01$

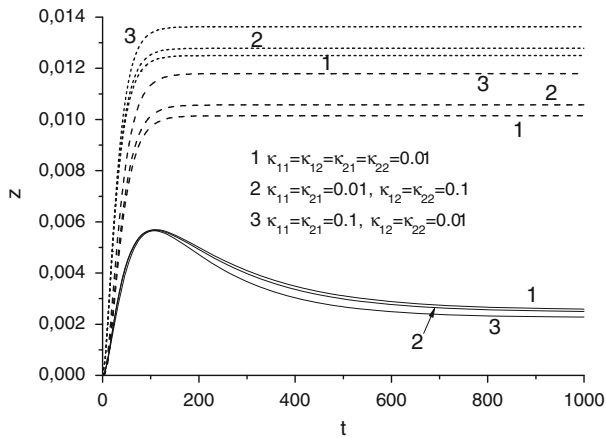


**Fig. 5** Dependence of the turnover rate  $z(t)$  determined by Eqs. (1)–(4) with  $a_1 = a_2 = 1$  at the surface  $S_2$  on the parameters  $\kappa_{ij}$  and  $k_{ij}, i, j = 1, 2$ , in the case  $s_1 = s_2 = 1, k_1 = k_2 = 0$  and  $\lambda = 0.1$ .  $k_{11} = k_{22} = 0.0166, k_{12} = k_{21} = 0$ —solid line,  $k_{11} = k_{21} = 0.0166, k_{12} = k_{22} = 0$ —dashed line,  $k_{11} = k_{12} = k_{21} = k_{22} = 0.0166$ —short dashed line

Figure 4 depicts the dependence of  $z$  on  $\lambda_{i,jn}$  for  $k_1 = k_2 = 0$  and  $k_{11} = k_{21} = 1.66 \times 10^{-2}$  in the case where both reactants adsorb on the inactive interval  $(x_*, 1)$ , i.e.  $k_{12} = k_{22} = 0$ . We observe that, for all  $t > 0, z$  increases as the jump rates,  $\lambda_{2,11} = \lambda_{2,21}$ , of both reactants from the inactive position  $x_* + 0$  into the active vacant location  $x_* - 0$  grows. Curves 3 and 4 show that this behaviour of  $z$  is not true if only the jump rate  $\lambda_{2,21}$  of reactant  $A_2$  increases.

In Fig. 5, we compare dynamics of  $z$  for  $\lambda = 0.1$  and  $k_1 = k_2 = 0$  in all three adsorption cases of reactants  $A_1$  and  $A_2$  ( $k = 1.66 \times 10^{-2}; k_{12} = k_{21} = 0, k_{11} = k_{22} = 1.66 \times 10^{-2}; k_{12} = k_{22} = 0, k_{11} = k_{21} = 1.66 \times 10^{-2}$ ). In each case we compare

the turn-over rate  $z$  corresponding to  $\kappa = 0.01$ ;  $\kappa_{11} = \kappa_{21} = 0.01$ ,  $\kappa_{12} = \kappa_{22} = 0.1$ ; and  $\kappa_{11} = \kappa_{21} = 0.1$ ,  $\kappa_{12} = \kappa_{22} = 0.01$ . We observe a similar behaviour of  $z$  in cases where  $A_1$  and  $A_2$  adsorb only on the inactive interval or were each reactant adsorbs on both intervals. Figure 5 shows that in these two adsorption cases the increase of the diffusivity  $\kappa_{11} = \kappa_{21}$  in the inactive interval determines larger values of  $z$  compared to those corresponding to the same increase of the reactants diffusivity  $\kappa_{12} = \kappa_{22}$  in the active interval. In the case where  $A_1$  adsorbs on the inactive interval and  $A_2$  on the active one, the increase of the diffusivity  $\kappa_{11} = \kappa_{21}$  in the inactive interval decreases  $z$  and determines values of  $z$  that are smaller those corresponding to the same increase of the diffusivity  $\kappa_{12} = \kappa_{22}$  in the active interval (see solid lines in this figure).

### 3.2 Numerical results of system (1)–(7)

Numerical results are presented in Figs. 6, 7, 8 and 9.

Figure 6 depicts the increase of  $z$  as  $x_*$  decreases in the case  $k = 1.66 \times 10^{-2}$ ,  $k_1 = k_2 = 0$ ,  $\kappa = \lambda = 0.5$ . This result is similar to that illustrated in Fig. 1 for system (1)–(4) with given  $a_1 = a_2 = 1$  at the surface  $S_2$ .

From Fig. 7 we see that, for  $k = 1.66 \times 10^{-2}$ ,  $k_1 = k_2 = 0$ ,  $\kappa = 0.01$  and small  $t$ , the increase of  $\lambda$  increases  $z$ . For large  $t$ , function  $z$  behaves vice-versa. Similarly, for  $\lambda = 0.01$  and small  $t$ , function  $z$  increases as  $\kappa$  grows but, for large  $t$ , its behaviour is opposite. Moreover, for large  $t$ ,  $z$  decreases to zero, because concentrations  $a_1(t, x)$  and  $a_2(t, x)$  tend to zero. For comparison we also present dynamics of  $z$  determined by Eqs. (1)–(4) with given  $a_1$  and  $a_2$  at the surface  $S_2$ . In this case  $z$  increases for all  $t > 0$  as  $\lambda$  or  $\kappa$  increases.

Figure 8 presents the comparison of  $z$  dynamics for  $\lambda = 0.1$  and  $k_1 = k_2 = 0$  in three adsorption cases of  $A_1$  and  $A_2$ . If each reactant adsorbs on both active and inactive interval or both reactants adsorb only on the inactive interval then, for small  $t$ , the increase of diffusivity  $\kappa_{11} = \kappa_{21}$  of both reactants in the inactive interval increases

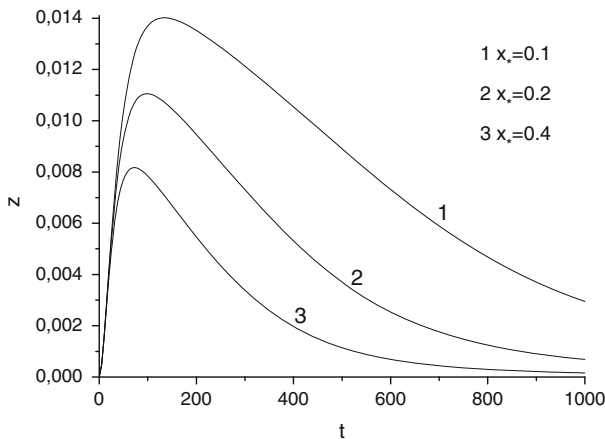


**Fig. 6** Influence of the active interval length  $x_*$  on the turnover rate  $z(t)$  determined by system (1)–(7) with densities  $a_1^0(x_1, x_2) = a_2^0(x_1, x_2) = 1$  and  $s_1 = s_2 = 1$  in the case  $k_1 = k_2 = 0$ ,  $\kappa = 0.5$  and  $\lambda = 0.5$

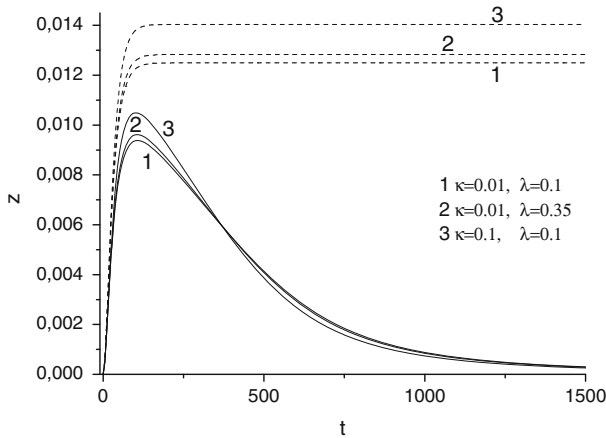


**Fig. 7** Dependence of the turnover rate  $z(t)$  determined by Eqs. (1)–(4) with  $a_1(t, x_1, 0) = a_2(t, x_1, 0) = 1$  (dashed line) and by system (1)–(7) with densities  $a_1^0(x_1, x_2) = a_2^0(x_1, x_2) = 1$  (solid line) on parameters  $\kappa$  and  $\lambda$  in the case  $s_1 = s_2 = 1$  and  $k_1 = k_2 = 0$

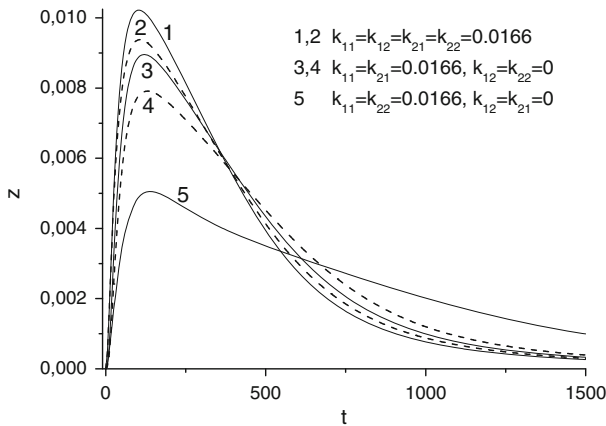


**Fig. 8** Effect of increasing parameters  $k_{ij}$  and  $\kappa_{ij}$ ,  $i, j = 1, 2$ , on the turnover rate  $z(t)$  determined by system (1)–(7) with densities  $a_1^0(x_1, x_2) = a_2^0(x_1, x_2) = 1$  and  $s_1 = s_2 = 1$  in the case  $k_1 = k_2 = 0$  and  $\lambda = 0.1$ .  $\kappa_{11} = \kappa_{21} = 0.1, \kappa_{12} = \kappa_{22} = 0.01$ —solid line,  $\kappa_{11} = \kappa_{12} = \kappa_{21} = \kappa_{22} = 0.01$ —dashed line

$z$ . For large  $t$ , its influence is opposite. Simulations show that the increase of the diffusivity  $\kappa_{12} = \kappa_{22}$  of both reactants in the active interval also increases  $z$  for small  $t$  but this increase is smaller than that corresponding to the same diffusivity increase in the inactive interval. Curve 5 in this figure corresponds to the case where  $A_1$  and  $A_2$  adsorb on the inactive and active interval, respectively. For small  $t$ , values of  $z$  are smaller than those corresponding to the other two adsorption cases, but for large  $t$  its values are larger.

In Fig. 9, we compare the total amount of product  $B$  at time  $t$ ,  $I_b = \int_0^1 dx_1 \int_0^1 b dx_2$ , for  $k = 0.1, \kappa = 0.5, \lambda = 0.5$  in cases where  $s_1 = s_2 = 1; s_2 = s_1(1/x_* - 1), s_1 = 1$  and  $x_* = 0.1, 0.2, 0.4$ . In the case  $s_1 = s_2 = 1$ , function  $I_b$  grows as  $x_*$  increases,

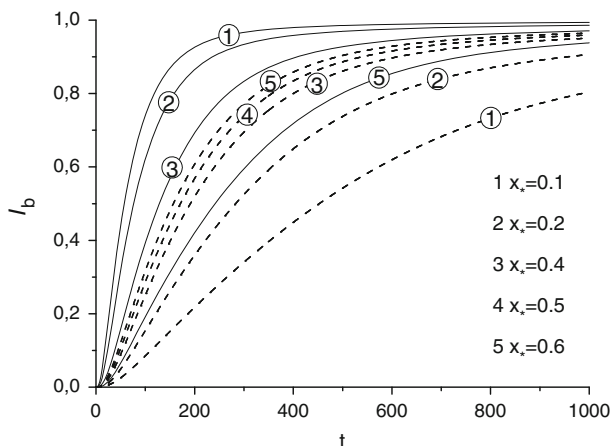


**Fig. 9** Dependence of the total amount of the product  $I_b$  on the active interval length  $x_*$  in the case  $a_1^0(x_1, x_2) = a_2^0(x_1, x_2) = 1, k_1 = k_2 = 0, k = 0.1,$  and  $\lambda = 0.5, \kappa = 0.5. s_1 = s_2 = 1$ —dashed line,  $s_1 = 1, s_2 = s_1(1/x_* - 1)$ —solid line

but, in the other one,  $I_b$  decreases as  $x_*$  increases. In both cases of the  $s_1$  and  $s_2$  distribution, values of  $I_b$  coincide for  $x_* = 0.5$ .

### 4 Conclusions

To conclude the paper, we summarise the main results. In this paper, using a phenomenological (mean-field) model in two-dimensional space we studied numerically bimolecular surface reactions proceeding on supported catalysts coupled with both reactants and product bulk diffusion in a bounded impermeable vessel. The model includes the adsorption, desorption, surface diffusion of adsorbed particles of each reactant, and rapid product desorption from the surface. Two different arrangements of adsorption sites were used and three cases of both reactants adsorption on them are considered: (i) each reactant can adsorb on both active catalyst particle and inactive support, (ii) one of the reactants  $A_1$  and  $A_2$  adsorbs on the catalyst particle while the other one adsorbs on the inactive in reaction support, (iii) both reactants adsorb only on the inactive support.

Inactive in reaction sites, due to possibility of adsorption of at least one of reactants and diffusion of adsorbed particles on them, constitute an additional (to the adsorption) channel transporting particles onto active ones. In case (i) of reactants adsorption, we have the adsorption channel of both reactants and the spillover one of both reactants from the inactive interval onto the active one. In case (ii), we have the adsorption channel of reactant  $A_2$  and the spillover one of  $A_1$ . At last, in case (iii), both reactants are transported onto active interval by the spillover channel.

The main characteristic we studied was the catalyst particle specific conversion rate (turn-over rate) of molecules of both reactants into the product ones. We analysed the effects of spillover on the turn-over rate under different conditions and demonstrated that:

1. The ER step remarkably increases the turn-over rate  $z$  compared to that corresponding to only one LH mechanism. Function  $z$  determined by system (1)–(4) with given values of  $a_1$  and  $a_2$  at the surface  $S_2$  is monotonic in time for  $k_1 = k_2 \geq 0$  and non-monotonic if only one of  $k_1$  and  $k_2$  is zero.
2. The size of the active interval strongly influence the turn-over rate. In both cases of active sites arrangement,  $z$  determined by Eqs. (1)–(4) with given  $a_1$  and  $a_2$  at the surface  $S_2$  or system (1)–(7) grows as size  $x_*$  decreases. Moreover, values of  $z$  corresponding to the case  $s_2 = s_1(\frac{1}{x_*} - 1)$ ,  $s_1 = 1$  are larger than those corresponding to the case  $s_1 = s_2 = 1$ .
3. The increase of at least one of diffusion coefficients  $\kappa_{ij}$  increases  $z$  determined by system (1)–(7) or Eqs. (1)–(4) with given concentrations  $a_1$  and  $a_2$  at the surface  $S_2$ .
4. In the case where one of reactants adsorbs on the inactive interval and the other on the active one,  $s_1 = s_2$ , and  $k_1 = k_2 = 0$ , the steady-state value of  $z$  determined by system (1)–(4) with given  $a_1 = a_2$  at the surface  $S_2$  possesses a maximum at some value  $\lambda_*$ , e.g.  $\lambda_* \approx 0.055$  for  $k_{11} = k_{22} = 0.0166$ ,  $k_{12} = k_{21} = 0$ ,  $\kappa = 0.01$ .
5. In the case, where both reactants adsorb only on the inactive support, the turn-over rate  $z$  is a monotonically increasing function in time.
6.  $z$  determined by system (1)–(7) is non-monotonic in time. It attains a maximum value and then tends to zero as time grows. Moreover,  $z$  grows only for small  $t$  as  $\kappa$ ,  $\kappa_{11} = \kappa_{21}$ , or  $\lambda$  increase and behaves vice versa for large  $t$ .
7. Values of the total amount of product  $B$  for  $s_1 = s_2 = 1$  monotonically increase as size of the active interval,  $x_*$ , grows and decrease for  $s_2 = s_1(1/x_* - 1)$ ,  $s_1 = 1$ .

Results of simulations let us to think that the phenomenological model presented here is able to describe qualitatively processes that proceed at constant temperature during monomer–monomer reactions on supported catalysts.

**Acknowledgments** This work was supported by the Research Council of Lithuania (Project No. MIP-052/2012).

## References

1. D.Y. Murzin, *Ind. Eng. Chem. Res.* **44**, 1688 (2005)
2. T.G. Mattos, F.D.A. Aarão Reis, *J. Catal.* **263**, 67 (2009)
3. L.J. Broadbelt, R.Q. Snurr, *Appl. Catal. A* **200**, 23 (2000)
4. V.P. Zhdanov, B. Kasemo, *Surf. Sci. Rep.* **39**, 25 (2000)
5. H. Lynggaard, A. Andreassen, C. Stegelmann, P. Stoltze, *Prog. Surf. Sci.* **77**, 71 (2004)
6. V.P. Zhdanov, B. Kasemo, *J. Catal.* **170**, 377 (1997)
7. L. Cwiklik, B. Jagoda-Cwiklik, M. Frankowicz, arXiv:physics/0409153v2[physics.chem-ph], 20 Jan 2005
8. T.G. Mattos, F.D.A. Aarão Reis, arXiv:0906.3063v[cond-mat.stat-mech] 17 Jun 2009
9. L. Cwiklik, B. Jagoda-Cwiklik, M. Frankowicz, *Appl. Surf. Sci.* **252**, 778 (2005)
10. W.C. Conner, J.L. Falconer, *Chem. Rev.* **95**, 759 (1995)
11. J. Libua, H.-J. Freund, *Surf. Sci. Rep.* **57**, 157 (2005)
12. R. Piccolo, C.R. Henry, *Appl. Surf. Sci.* **162**, 670 (2000)
13. H. Chen, H. Yang, Y. Briker, C. Fairbridge, O. Omotoso, L. Ding, Y. Zheng, *Z. Ring, Catal. Today* **125**, 256 (2007)
14. K. Polychronopoulou, A.M. Efstathiou, *Catal. Today* **116**, 341 (2006)
15. A. Kecskemeti, T. Bansagi, F. Solymosi, *Catal. Lett.* **116**, 101 (2007)

16. M. Laurin, V. Johaneck, A.W. Grant, B. Kasemo, J. Libua, H.-J. Freund, J. Chem. Phys. **123**, 054701 (2005)
17. E. Odier, Y. Schuurman, C. Mirodatos, Catal. Today **127**, 230 (2007)
18. R. Marques, S. Capela, S. DaCosta, F. Delacroix, G. Djega-Mariadassou, P. Da Costa, Catal. Commun. **9**, 1704 (2008)
19. M. Bowker, E. Fourre, Appl. Surf. Sci. **254**, 4225 (2008)
20. L. Cwiklik, B. Jagoda-Cwiklik, M. Frankowicz, Surf. Sci. **572**, 318 (2004)
21. E.V. Kovaliov, E.D. Resnyanskii, V.I. Elokhin, B.S. Bal'zhinimaev, A.V. Myshlyatsev, Phys. Chem. Chem. Phys. **5**, 784 (2003)
22. L. Cwiklik, arXiv:0710.4785v1 [cond-mat.mtrl-sci] 25 Oct 2007
23. L. Cwiklik, Chem. Phys. Lett. **449**, 304 (2007)
24. V. Skakauskas, P. Katauskis, J. Math. Chem. **51**, 492 (2013)
25. V. Skakauskas, P. Katauskis, J. Math. Chem. **51**, 1654 (2013)
26. A.A. Samarskii, *The Theory of Difference Schemes* (Marcel Dekker, New York, 2001)